Developmental Biology 387 (2014) 109–120

Contents lists available at ScienceDirect

Developmental Biology

journal homepage: www.elsevier.com/locate/developmentalbiology

Sox17 is required for normal pulmonary vascular morphogenesis

Alexander W. Lange [a], Hans Michael Haitchi [c], Timothy D. LeCras [a], Anusha Sridharan [a], Yan Xu [a], Susan E. Wert [a], Jeanne James [b], Nicholas Udell [d], Philipp J. Thurner [d], Jeffrey A. Whitsett [a,*]

[a] Perinatal Institute, Division of Pulmonary Biology, Cincinnati Children's Hospital Medical Center, The University of Cincinnati College of Medicine, 3333 Burnet Avenue, Cincinnati, OH 45229-3039, United States
[b] Heart Institute, Department of Pediatrics, Cincinnati Children's Hospital Medical Center and the University of Cincinnati College of Medicine, Cincinnati, OH 45229-3039, United States
[c] Clinical and Experimental Sciences, Faculty of Medicine, and National Institute for Health Research Respiratory Biomedical Research Unit, Southampton General Hospital, United Kingdom
[d] Bioengineering Sciences Research Group, Faculty of Engineering and the Environment, University of Southampton, United Kingdom

ARTICLE INFO

Article history:
Received 3 May 2013
Received in revised form
14 November 2013
Accepted 16 November 2013
Available online 10 January 2014

Keywords:
Sox17
Lung
Endothelial
Vascular morphogenesis
Dermo1-Cre

ABSTRACT

The SRY-box containing transcription factor Sox17 is required for endoderm formation and vascular morphogenesis during embryonic development. In the lung, Sox17 is expressed in mesenchymal progenitors of the embryonic pulmonary vasculature and is restricted to vascular endothelial cells in the mature lung. Conditional deletion of *Sox17* in splanchnic mesenchyme-derivatives using *Dermo1-Cre* resulted in substantial loss of Sox17 from developing pulmonary vascular endothelial cells and caused pulmonary vascular abnormalities before birth, including pulmonary vein varices, enlarged arteries, and decreased perfusion of the microvasculature. While survival of *Dermo1-Cre*;*Sox17Δ/Δ* mice (herein termed *Sox17Δ/Δ*) was unaffected at E18.5, most *Sox17Δ/Δ* mice died by 3 weeks of age. After birth, the density of the pulmonary microvasculature was decreased in association with alveolar simplification, biventricular cardiac hypertrophy, and valvular regurgitation. The severity of the postnatal cardiac phenotype was correlated with the severity of pulmonary vasculature abnormalities. Sox17 is required for normal formation of the pulmonary vasculature and postnatal cardiovascular homeostasis.

Introduction

The pulmonary vasculature consists of an elaborate network of arteries, capillaries, and veins required for blood–gas exchange. Formation of the pulmonary vascular network from mesenchymal progenitors is initiated concurrently with branching morphogenesis of the respiratory epithelium in the embryonic lung, and interdependent tissue interactions between the developing pulmonary vasculature and respiratory epithelium guide their respective growth and maintenance. Both vasculogenesis, the de novo formation of blood vessels from endothelial cell precursors, and angiogenesis, the sprouting of new vessels from the existing vasculature, contribute to pulmonary vascular development (Galambos and deMello, 2007). While the extent to which each process contributes to formation of the pulmonary vascular network is debated, ultimately precise regulation of vessel remodeling is required for integration of the macro- and microvascular networks to ensure normal pulmonary vascular blood flow. While a number of pathways are known to mediate formation of the pulmonary vasculature, the molecular mechanisms that govern pulmonary vascular morphogenesis in the embryonic lung remain poorly understood. Formation of the pulmonary microvasculature and the larger drainage vessels is critical for cardiovascular function and gas exchange after birth. Dramatic increases in pulmonary blood flow and a marked decrease in pulmonary vascular resistance accompany the transition to a closed circulatory system and adaptation to air breathing at birth. The decrease in pulmonary vascular resistance after birth is dependent upon the proper formation of the pulmonary vasculature and is required for normal postnatal cardiovascular function.

Sox17 is a member of subgroup F of the Sry-related high mobility group box (SoxF) family of transcription factors, and is required for endoderm formation, pancreatobiliary organ segregation, and the establishment and maintenance of fetal/neonatal hematopoietic stem cells from haemogenic endothelium (Clarke et al., 2013; Kanai-Azuma et al., 2002; Kim et al., 2007; Spence et al., 2009). Sox17 and closely related SoxF factors (Sox7 and Sox18) have redundant functions during vascular development. Sox18 is required for formation of the lymphatic vasculature in mice and mutations in *SOX18* are the underlying cause of

* Corresponding author. Fax: +1 513 636 7868.
E-mail address: Jeffrey.Whitsett@cchmc.org (J.A. Whitsett).

0012-1606/$ - see front matter © 2014 Elsevier Inc. All rights reserved.
http://dx.doi.org/10.1016/j.ydbio.2013.11.018

hypotrichosis–lymphedema–telangiectasia in humans (Francois et al., 2008; Irrthum et al., 2003). While germline deletion of *Sox17* results in embryonic lethality by E10.5 due to the loss of definitive endoderm, mutant mice display heart-looping defects and enlarged cardinal veins during early cardiovascular development (E8.0–8.75) (Kanai-Azuma et al., 2002; Sakamoto et al., 2007). Endothelial-specific deletion of *Sox17* in embryonic or perinatal mice caused hematopoietic stem cell deficiencies, in utero lethality, and defects in arterial differentiation and vascular formation (Clarke et al., 2013; Corada et al., 2013; Kim et al., 2007). In adult mice, Sox17 regulates endothelial cell proliferation, sprouting, and migration to promote tumor angiogenesis (Yang et al., 2013). Inhibition of *Sox18* and *Sox7* in zebrafish demonstrated that these genes cooperate in arteriovenous specification (Cermenati et al., 2008; Herpers et al., 2008; Pendeville et al., 2008), and *Sox17*/*Sox18* double knockout mice have anterior dorsal aorta and head/cervical microvascular abnormalities (Sakamoto et al., 2007). Angiogenesis in the postnatal liver and kidney is defective in $Sox17^{+/-}$;$Sox18^{-/-}$ mice, causing death of approximately half of the compound mutant mice by postnatal day 21 (Matsui et al., 2006). While these studies demonstrate important roles for SoxF genes in vascular development, early embryonic lethality of knockout mice and functional redundancy has precluded the study of their role in the formation of the pulmonary vasculature.

The present study identifies the role of Sox17 during pulmonary vascular morphogenesis. In the lung, Sox17 expression was restricted to endothelial cells of the developing pulmonary vasculature. Conditional deletion of *Sox17* in the splanchnic mesenchyme-derivatives using *Dermo1Cre* (*Sox17Δ/Δ* mice) caused dilation of the larger pulmonary arteries and veins and impaired formation and/or maintenance of the pulmonary microvasculature. The majority of *Sox17Δ/Δ* mice died by 3 weeks of age, with the severity of pulmonary vascular abnormalities correlating with the development of dilated cardiomyopathy. These findings demonstrate that Sox17 is required for normal pulmonary vascular morphogenesis and postnatal cardiopulmonary function.

Materials and methods

Mice

$Sox17^{flx}$ mice (Sv/129 background), in which exons 3–5 are flanked by loxP sites, were generated in this laboratory and have been previously described (Spence et al., 2009). *Dermo1-Cre* mice ($Twist2^{tm1.1(cre)Dor}$; C57BL/6J background) were kindly provided by Dr. David Ornitz (Washington University, St. Louis, MO) (Yu et al., 2003). $Sox17^{GFP}$ reporter knock-in mice were kindly provided by Dr. Sean Morrison (University of Texas Southwestern, Dallas, TX) (Kim et al., 2007). *Dermo1-Cre*;$Sox17^{flx/flx}$ (*Sox17Δ/Δ*) mice were generated by *Dermo1-Cre*;$Sox17^{+/flx}$ and $Sox17^{flx/flx}$ breedings and the presence of a copulation plug in the morning represented embryonic day (E) .5 for timed matings. Genotypes were determined by PCR using genomic tail DNA and primers for *Cre* and the *Sox17* wild-type and floxed alleles (Spence et al., 2009). Pregnant dams were sacrificed by CO_2 inhalation and embryonic mice were harvested at indicated times. Postnatal mice were sacrificed by anesthesia using a mixture of ketamine, aceprozamine, and xylazine and exsanguination by severing the inferior vena cava and descending aorta. Animals were housed in pathogen-free conditions according to protocols approved by the Institutional Animal Care and Use Committee at Cincinnati Children's Hospital Research Foundation.

Immunohistochemistry and immunofluorescence

Embryos harvested from timed matings were fixed by immersion and lungs from postnatal mice were inflation fixed using 4% paraformaldehyde (PFA) in phosphate-buffered saline (PBS). Following overnight immersion in 4% PFA/PBS, fixed tissue was processed according to standard protocols for paraffin or frozen embedding. Hematoxylin and eosin (H&E) staining, immunohistochemistry, and immunofluorescence were performed on tissue sections (5–10 μm) as previously described (Lange et al., 2009). Primary antibodies included guinea pig anti-Sox17 (Seven Hills Bioreagents), goat anti-endomucin (R&D Systems), rat anti-Pecam-1 (BD Pharmingen), GSL-IB4-biotin (Vector Labs), rat anti-CD34 (Abcam), goat anti-EphB4 (R&D Systems), and mouse anti-alpha smooth muscle actin (Sigma). Fluorophore-conjugated secondary antibodies included Alexa Fluor-488 and Alexa Fluor-594 (Jackson ImmunoResearch and Life Technologies). For fluorescent stains, sections were stained with DAPI and mounted with ProLong Gold anti-fade reagent following antibody labeling (Invitrogen). Brightfield images were obtained using a Zeiss Axio ImagerA2 microscope equipped with AxioVision Software. Fluorescent images were obtained using a Nikon A1Rsi inverted laser confocal microscope and analyzed using Imaris software (Bitplane Scientific Software).

Whole mount immunofluorescence

Lungs from 2 week old mice were inflation fixed with 4% PFA/PBS cryoprotected in sucrose/PBS, and embedding in OCT compound (TissueTek). Thick sections (150 μm) of lung tissue were cut with a cryostat and stained using a whole mount immunofluorescence protocol (Ahnfelt-Ronne et al., 2007). Primary antibodies included goat anti-endomucin (R&D Systems) and mouse anti-alpha smooth muscle actin (Sigma), and secondary antibodies were Alexa Fluor-488 and Alexa Fluor-594. Following antibody labeling, sections were stained with DAPI and mounted on slides for imaging. A Nikon A1Rsi inverted laser confocal microscope was used to acquire 2×2 z-stack tile scans. Fluorescent images were analyzed using Imaris software and endomucin staining threshold intensities were used to generate surface representations of the pulmonary vascular network and quantify the area and volume of the lung vasculature.

Micro-computed tomography

Control ($n=5$) and *Sox17Δ/Δ* ($n=10$) embryos harvested at E18.5 were euthanized and immersion fixed in 4% PFA/PBS. Whole embryos were immersed in 25% Lugol's iodine solution (100% Lugol's; 10 g KI, 5 g I_2 in 100 ml H_2O) for 48 h prior to micro-computed tomography (microCT) scanning [adapted from Degenhardt et al. (2010)]. Images were obtained using a microCAT II microCT using a kVp of 80 and an anode current of 225 μA (CCHMC Imaging Research Center). Projections ($n=776$) were collected through 194° of gantry rotation using an X-ray exposure time of 2.30 s and a bin factor of 2. The set of projections was reconstructed using COBRA (cone beam reconstruction algorithm, Exxim Computing Corporation, Pleasanton, CA, USA). The reconstructed image voxel size was 19.7 μm isotropic. The raw CT slice data were converted to DICOM format and processed using OsiriX software (Pixmeo, Geneva, Switzerland).

Endothelial cell enrichment and RNA analysis

To isolate pulmonary endothelial cells, E18.5 lungs harvested from control ($n=7$) and *Sox17Δ/Δ* ($n=5$) embryos were minced with microdissection knives and placed in digestion medium

(Hank's Balanced Salt Solution, .05% trypsin, .1% collagenase, 25 μm HEPES) at 37 °C for 1 h. Lung digestion was stopped by the addition of DMEM with 10% fetal bovine serum. Cells were passed through a 40 μm nylon mesh strainer into a 60 mm sterile dish and transferred to a 15 ml tube. Following centrifugation at 300–400*g*, 10 min, the supernatant was discarded and cell pellets were washed with HBSS. Cells were centrifuged as before and pellets were resuspended in 90 μl autoMACS Running Buffer and 10 μl CD146-conjugated MicroBeads (Miltenyi Biotec). After incubating for 15 min with rotation at 4 °C, 910 μl of autoMACS Running Buffer was added, cells were centrifuged as before, and the supernatant was aspirated. Cells were resuspended in 500 μl of Running Buffer and passed through a 40 μm nylon filter cap into a round bottom tube prior to sorting using an AutoMACS Pro Separator to isolate CD146-positive (endothelial-enriched) and negative (non-endothelial) cell populations (Miltenyi Biotec). Total RNA was isolated from CD146-positive and negative cells using a RNeasy Micro Kit (Qiagen), and reverse transcription reactions were performed using an iScript cDNA synthesis kit (BioRad) according to manufacturer's recommendations. Microarray analysis was performed using RNA isolated from CD146-positive cells from control and *Sox17Δ/Δ* embryo lungs and Mouse Gene 1.0 ST Arrays (Affymetrix, Santa Clara, CA). qPCR was performed using a StepOnePlus Real-Time PCR System and TaqMan gene expression assays (Applied Biosystems). Relative expression was calculated using the delta-delta Ct method and statistical significance was determined by two-tailed unpaired Student's *t*-test using Prism6 GraphPad Software ($p \leq .05$).

Echocardiography and heart measurements

Echocardiography was performed on 2 week old control ($n=7$) and *Sox17Δ/Δ* ($n=10$) mice. Mice were anaesthetized using 1.5% isoflurane and oxygen with anesthesia maintained during assessment using a nose cone. A Vevo2100 (VisualSonics) echocardiography system equipped with a 40 MHz transducer was used to evaluate left ventricular dimensions and function using M-mode imaging. Both pulsed wave and color Doppler imaging were used to assess valve function with the addition of tissue Doppler imaging of the mitral valve (MV) annulus as a noninvasive indicator of left ventricular (LV) diastolic function (Acehan et al., 2011). For measuring ventricle weights, hearts were removed from 2 week old control ($n=10$) and *Sox17Δ/Δ* ($n=4$) mice and dissected to isolate the free wall of the right ventricle (RV) from the left ventricle and septum (LV+S). The ratios of the RV and LV+S weight to body weight (RV:BW and LV+S:BW) were used as indexes of cardiac hypertrophy.

Results

Sox17 is expressed in developing pulmonary vascular endothelial cells

Multiple cell types are derived from the mesenchyme of the developing lung, including fibroblasts, pericytes, smooth muscle, and endothelial cells that contribute to the pulmonary vasculature. Sox17 is expressed in the embryonic and adult lung at sites consistent with nascent and mature endothelial cells (Lange et al., 2009). To determine whether Sox17 expression in the developing lung is restricted to endothelial cells, lung sections from E12.5, E14.5, and E18.5 embryos were co-stained for Sox17 and the endothelial-specific markers, endomucin and Pecam-1. Sox17 staining was detected in the nucleus of endothelial cells labeled with endomucin and Pecam-1 in the developing lung at each embryonic stage (Fig. 1A–F). *Sox17^{GFP}* knock-in reporter mice, in which GFP is inserted into the endogenous *Sox17* coding region, were used to further assess Sox17 expression in the developing lung (Kim et al., 2007). In E18.5 *Sox17^{GFP}* mouse lungs, GFP was co-expressed with endomucin and Pecam-1 (Fig. 1G–L). At E18.5, Sox17 immunostaining and GFP-reporter expression were more strongly detected in arterial and microvascular endothelial cells compared to veins. While Pecam-1 broadly labels endothelial cells across all blood vessel types, endomucin becomes increasingly restricted to capillary and venous endothelial cells in mature vascular networks (Brachtendorf et al., 2001). Thus, in E18.5 mouse lungs Sox17/endomucin co-expressing cells were primarily detected to the peripheral microvasculature, whereas Sox17/Pecam-1 co-expressing cells were observed throughout the developing pulmonary vasculature (Fig. 1). These findings are consistent with the endothelial-specific expression of a *Sox17-mCherry* knock-in reporter during mouse lung development, as well as labeling of the endothelial cell lineage when Cre recombinase is inserted into the Sox17 locus (Burtscher et al., 2012; Choi et al., 2012; Engert et al., 2013; Engert et al., 2009; Liao et al., 2009). Although Sox17 is highly expressed in the endoderm and is required for endoderm formation prior to the emergence of the lung epithelial primordium, it is not detected in the respiratory epithelium thereafter (Fig. 1) (Choi et al., 2012; Engert et al., 2013; Lange et al., 2009). Together, these data demonstrate that Sox17 expression in the mesenchyme of the developing lung is restricted to vascular endothelial cells.

Conditional deletion of Sox17 causes pulmonary vascular malformations and postnatal lethality

Dermo1-Cre mice were used to conditionally delete *Sox17* in the developing lung mesenchyme (Spence et al., 2009; White et al., 2006; Yu et al., 2003). To determine the distribution of Cre-mediated recombination, *Dermo1-Cre* mice were crossed with *Rosa26R-LacZ* reporter mice. X-gal staining and dual immunofluorescence for β-galactosidase and endomucin demonstrated widespread recombination in cells throughout the splanchnic mesenchyme of the developing lung of E18.5 *Dermo1-Cre/Rosa26R-LacZ* embryos, including endothelial cells lining the lumen of pulmonary arteries, veins, and microvasculature (Supplemental Fig. 1). *Dermo1-Cre* also directed recombination in the embryonic heart and at sites consistent with endothelial cells within the developing kidneys, intestine, and liver (Supplemental Fig. 1). In the heart, *Dermo1-Cre*-mediated recombination was detected in interstitial cells of the heart valves, the great vessels, and perivascular cells surrounding coronary vessels (Supplemental Fig. 1).

To determine the role of Sox17 in vascular morphogenesis in the embryonic lung, *Dermo1-Cre*;*Sox17$^{+/flx}$* mice were crossed with *Sox17$^{flx/flx}$* mice. Immunohistochemical staining of fetal and postnatal lungs demonstrated that Sox17 was selectively expressed in endothelial cells lining the lumen of pulmonary arteries and veins and throughout the peripheral microvasculature of the lung in control mice, with stronger Sox17 staining detected in arterial and microvascular endothelial cells compared to veins (Fig. 2C, E, and F). Immunostaining for Sox17 on lung sections from E18.5 *Sox17Δ/Δ* embryos demonstrated extensive, but variable loss of Sox17 in arterial, venous, and microvascular endothelial cells of the pulmonary vasculature (Fig. 2D, G, and H). Relatively rare Sox17-positive cells remained, indicating incomplete targeting of the pulmonary vascular endothelium by *Dermo1-Cre*. While genotypes of mice from *Dermo1-Cre*;*Sox17$^{+/flx}$* and *Sox17$^{flx/flx}$* matings harvested at E14.5 and E18.5 were observed at the expected Mendelian ratios, significantly fewer than expected *Dermo1-Cre*;*Sox17$^{flx/flx}$* mice (*Sox17Δ/Δ*) were observed at 3–4 weeks of age (8.4%, $p=.0003$; Table 1). Additionally, only 14% of the total expected number of *Sox17Δ/Δ* mice survived beyond 8 weeks

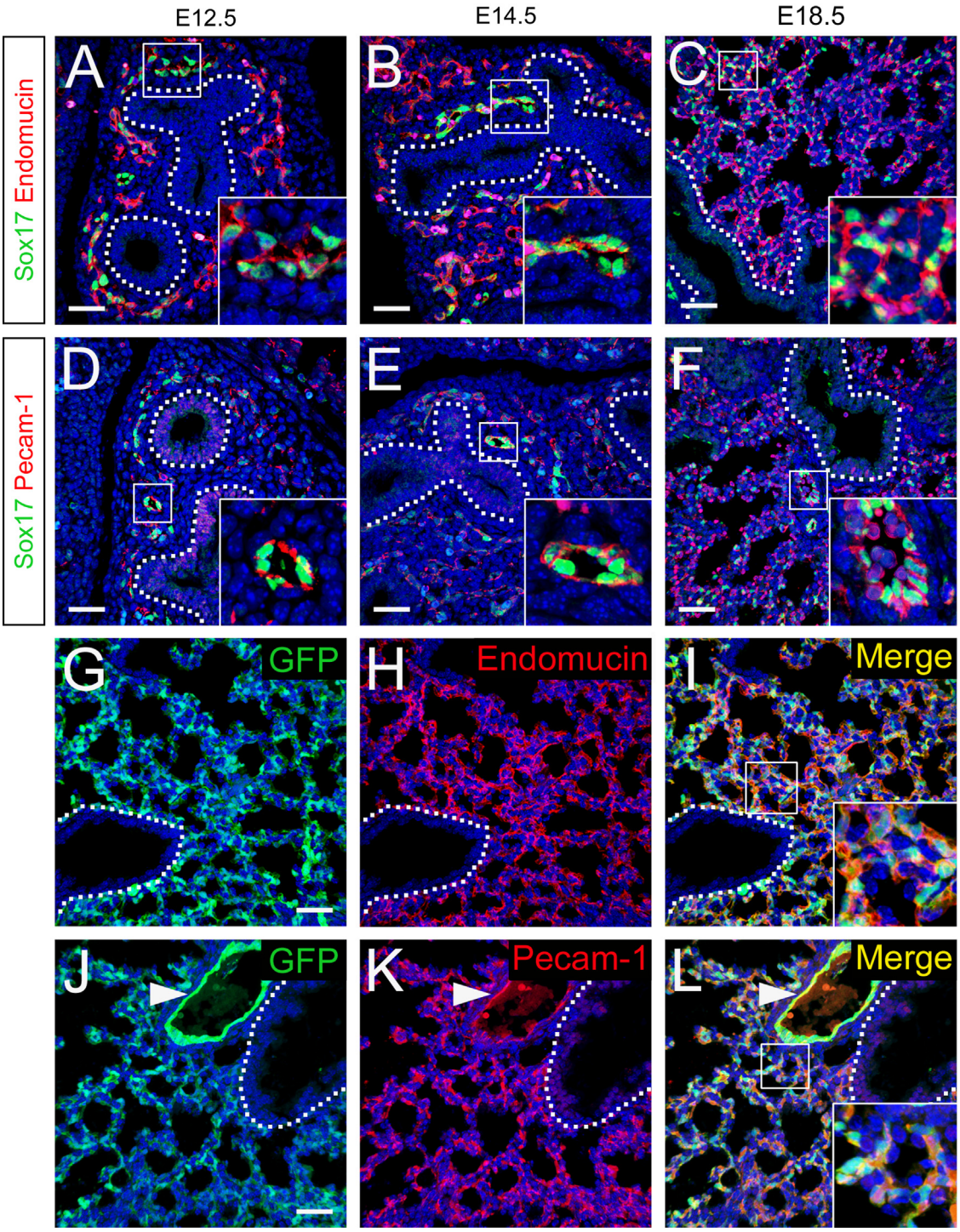

Fig. 1. Sox17 is expressed in endothelial cells in the developing lung. (A–F) Immunofluorescence double labeling for Sox17 (green) and endomucin (red, A–C) or Pecam-1 (red, D–F) was performed on sections from E12.5 (A and D), E14.5 (B and E), and E18.5 (C and F) mouse lungs. Sox17 was detected in the nuclei of cells staining for endothelial cell markers in the developing mouse lung. (G–L) Immunofluorescence for GFP (G and J) and endomucin (H) or Pecam-1 (K) was performed on sections from E18.5 *Sox17*^{GFP} reporter knock-in mouse lungs. Sox17-expressing cells labeled with the GFP reporter were co-stained with endothelial cell markers. Nuclei are stained with DAPI (blue). Insets show higher magnification of boxed regions and dotted lines denote the basal surface of the airway epithelium. Pulmonary artery (inset, F; arrowhead, J–L). Peripheral microvasculature (insets, C, I, and L). Red blood cell autofluorescence in panel F was masked using Imaris software. Scale bars 40 μm.

(5 of 35 expected). These data demonstrate that conditional deletion of *Sox17* with *Dermo1-Cre* causes variable postnatal lethality, with loss of 66% of *Sox17Δ/Δ* mice between birth and 3 weeks of age. Daily observation of neonatal mice from *Dermo1-Cre*;*Sox17*$^{+/flx}$ and *Sox17*$^{flx/flx}$ matings did not reveal any gross physical or behavioral abnormalities among the littermates that might predict their death. Thus, *Dermo1-Cre* efficiently deleted *Sox17* from endothelial cells in the developing lung vasculature and resulted in the sudden death of *Sox17Δ/Δ* mice in the postnatal period.

Since normal Mendelian ratios were observed at embryonic stages, control and *Sox17Δ/Δ* mice were examined at E18.5 to determine the effects of conditional deletion of *Sox17* on pulmonary vascular morphogenesis. While gross morphology of E18.5

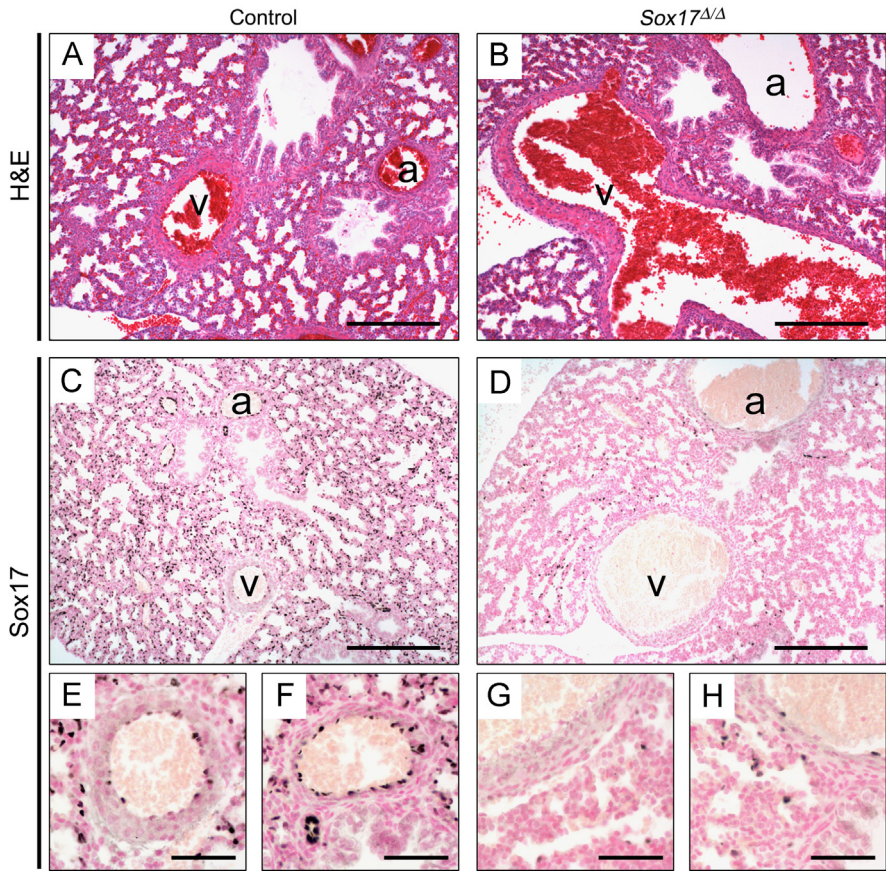

Fig. 2. Deletion of *Sox17* in the developing lung mesenchyme causes dilated pulmonary vessels. (A–B) H&E staining of tissue sections from E18.5 mouse lungs shows enlarged pulmonary vessels in *Sox17Δ/Δ* embryos (B) compared to controls (A). (C–H) Immunostaining for Sox17 on sections from E18.5 control (C, E, and F) and *Sox17Δ/Δ* (D, G, and H) lungs. *Dermo1-Cre* mediated deletion of *Sox17* results in the loss of Sox17 expression in the majority of arterial, venous, and microvascular endothelial cells in the developing lung. (E–H) Higher magnification images of arteries (F and H) and veins (E and G) shown in C and D. a, Artery; v, vein. Scale bars, 50 μm.

Table 1
Genotypes of mice from Dermo1Cre;$Sox17^{+/flx}$ × $Sox17^{flx/flx}$ matings.

Age	# Litters	Total mice	**Genotypes (%)**			
			$Sox17^{+/flx}$	$Sox17^{flx/flx}$	*Dermo1Cre; Sox17*$^{+/Δ}$	*Dermo1Cre; Sox17*$^{Δ/Δ}$
E14.5	7	46	9 (19.6%)	15 (32.6%)	12 (26.1%)	10 (21.7%)
E18.5	14	94	15 (16.0%)	29 (30.9%)	27 (28.7%)	23 (24.4%)
Adult	19	142	36 (25.3%)	43 (30.3%)	51 (36.0%)	12 (8.4%)*

* $p=.0003$; chi-square analysis.

littermates was indistinguishable and embryo length was unaffected, body weight of *Sox17Δ/Δ* mice was reduced 15% compared to control littermates (Supplemental Table 1). Histological analysis revealed enlarged macrovascular blood vessels (arteries and veins) in the lungs of E18.5 *Sox17Δ/Δ* embryos (Fig. 2). Vascular leak was not observed in the lungs of E18.5 *Sox17Δ/Δ* mice, indicating that vessel integrity was not compromised. At E18.5, formation of peripheral lung saccules was unaffected (Fig. 2) and no structural abnormalities were observed in other organs examined in *Sox17Δ/Δ* embryos, including the heart, liver, kidney, and gastrointestinal tract (data not shown).

To evaluate formation of the fetal vascular networks, including the pulmonary vasculature, E18.5 embryos were stained with Lugol's iodine solution and blood vessels were imaged using microCT. The developing pulmonary vascular network was visualized in 2D microCT slices (Fig. 3A and B), and in 3D renderings of whole lungs (Fig. 3C and D; Supplemental movies 1 and 2). Branching of the major pulmonary vessels into smaller arterioles and venules and the peripheral microvasculature was apparent in control embryos (Fig. 3A and C). In contrast, microCT images of lungs from *Sox17Δ/Δ* embryos showed marked enlargement of pulmonary arteries and veins (Fig. 3B and D). Staining of the peripheral microvasculature was also variably reduced in 40% of *Sox17Δ/Δ* mice (4/10) (Fig. 3B and D). Since Lugol's iodine selectively stains blood, it is unclear from these analyses whether the decreased staining intensity of the microvasculature represents reduced blood flow, structural abnormalities, or endothelial loss in the capillary network. Peripheral lung saccule formation was not affected in *Sox17Δ/Δ* embryos at E18.5 despite apparent defects in the pulmonary vasculature (Figs. 2 and 3). Quantitative analysis of microCT images demonstrated that the volume of pulmonary macrovasculature was significantly increased in *Sox17Δ/Δ* embryos (Supplemental Fig. 2). Abnormalities in pulmonary veins were more commonly observed than those in pulmonary arteries. While the number of abnormal lung vessels and the extent of dilation varied among *Sox17Δ/Δ* mice, enlarged veins located near the hilar region of the lung were the most frequently observed pulmonary vascular anomaly. MicroCT did not reveal any discernable abnormalities in the vasculature of other organs in E18.5 *Sox17Δ/Δ* embryos (Supplemental Fig. 3 and data not shown).

Pulmonary vein varix is a rare condition in humans that presents as an abnormal dilation of the pulmonary vein, typically near the lung hilum, with a normal entry into the left atrium (Benmenachem et al., 1975). Consistent with findings in pulmonary vein varix, the abnormally dilated pulmonary hilar veins in *Sox17Δ/Δ*

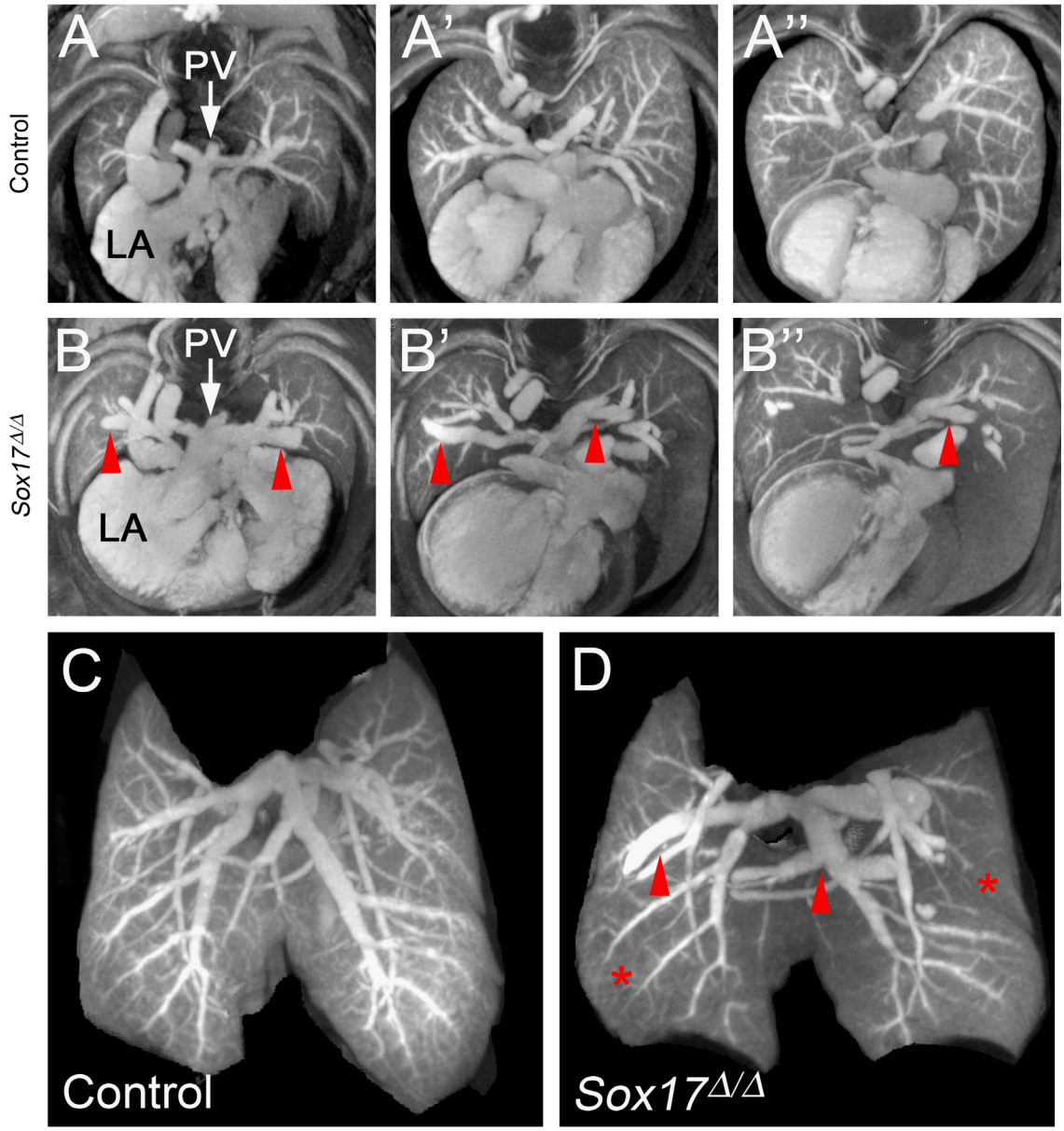

Fig. 3. MicroCT analysis shows pulmonary vascular abnormalities in *Sox17Δ/Δ* embryonic lungs. (A–B) MicroCT images comprised of a merged stack of 50 2D microCT slices. Panels depict a sequential series through the developing lungs of E18.5 control (A–A″) and *Sox17Δ/Δ* (B–B″) mice. Pulmonary veins were dilated (red arrowheads) and vascular branching was aberrant in the lungs of *Sox17Δ/Δ* embryos. (C–D) Static 3D images of the developing pulmonary vascular network in E18.5 control (C) and *Sox17Δ/Δ* (D) lungs showing dilated pulmonary blood vessels (red arrowheads) and reduced staining of the peripheral microvasculature (red asterisks). PV, pulmonary vein; LA, left atrium.

mice maintain a normal communication with the left atrium (Fig. 3B). Thus, conditional deletion of *Sox17* in the developing lung mesenchyme results in the formation of enlarged/dilated pulmonary blood vessels, including congenital pulmonary vein varices.

Pulmonary endothelial cell differentiation is not affected by conditional deletion of Sox17

To determine the effects of Sox17 deletion on differentiation of the developing pulmonary vascular endothelium, immunostaining was performed for markers of differentiated endothelial cells. The intensity of staining for GSL-IB4 (*Griffonia simplicifolia*, isolectin B4) and Pecam-1 in endothelial cells of pulmonary arteries and veins was similar in E18.5 control and *Sox17Δ/Δ* lungs, including endothelial cells lining the abnormally dilated vessels (Fig. 4). The intensity and distribution of Pecam-1 and CD34 staining in microvascular endothelial cells were unaltered in the lungs of *Sox17Δ/Δ* embryos, despite the widespread deletion of Sox17 from pulmonary microvasculature and hypoperfusion observed with microCT (Fig. 4C and F). Staining for EphB4 (Eph receptor B4), a marker of venous endothelial cells, demonstrated that both veins (EphB4-positive) and arteries (EphB4-negative) were enlarged in *Sox17Δ/Δ* embryo lungs (Fig. 4G and H). Formation of the lymphatic vasculature, as detected by LYVE-1 (lymphatic vessel endothelial hyaluronan receptor 1) staining, was unchanged in the lungs of *Sox17Δ/Δ* embryos (data not shown). Electron microscopy did not reveal any distinct ultrastructural abnormalities in the venous, arterial, or microvascular endothelium of E18.5 *Sox17Δ/Δ* embryos (data not shown). Thus, Sox17 is dispensable for endothelial cell differentiation in the developing lung, but is required for calibration of pulmonary blood vessel size during pulmonary vascular morphogenesis.

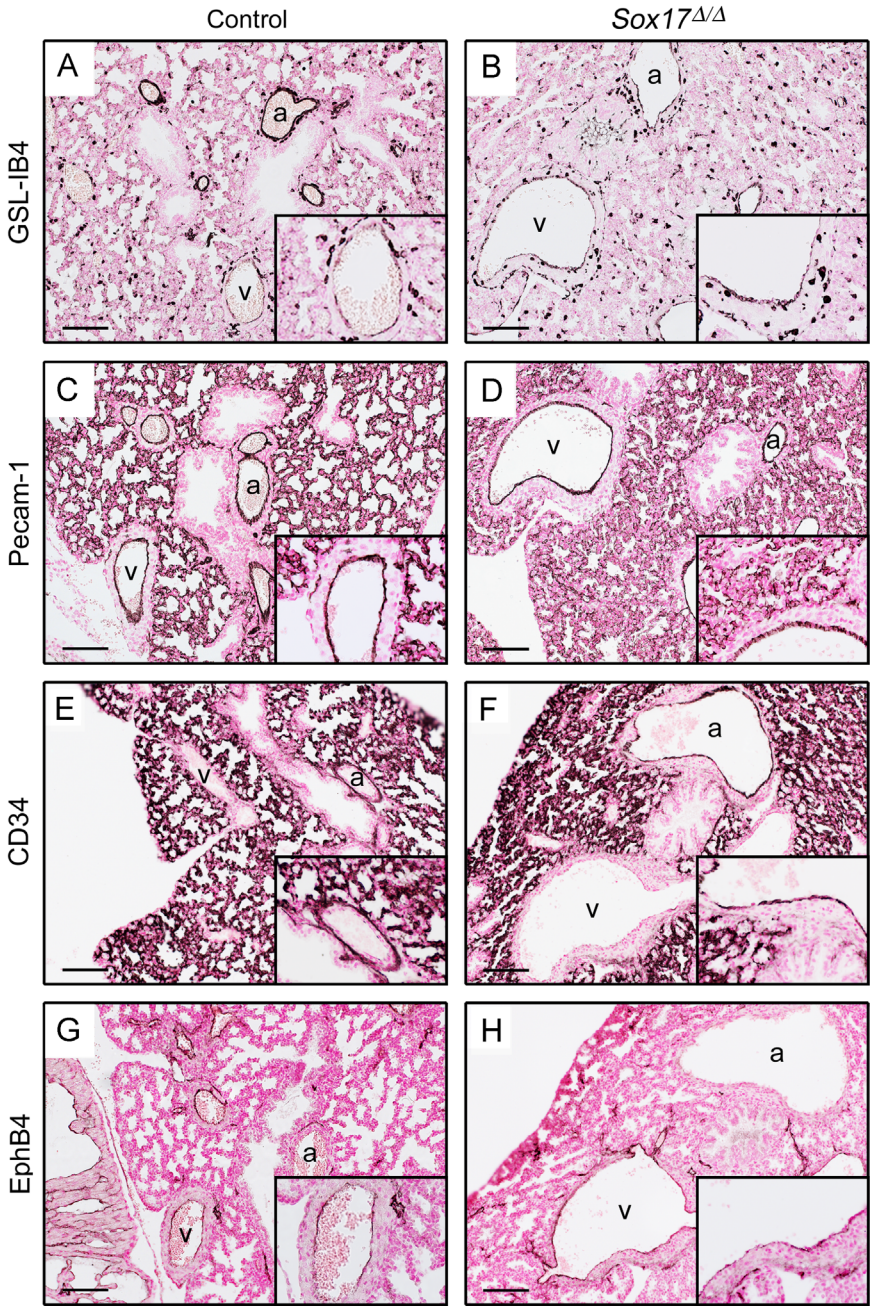

Fig. 4. Pulmonary vascular endothelial cell differentiation is not affected in *Sox17Δ/Δ* mouse lungs. Staining for GSL-IB4 (A–B), Pecam-1 (C–D), CD34 (E–F), and EphB4 (G–H) was performed on sections from E18.5 control (A, C, E, and G) and *Sox17Δ/Δ* (B, D, F, and H) lungs. No differences in staining for these endothelial cell markers were observed between control and *Sox17Δ/Δ* embryo lungs. (G–H) EphB4-positive veins and EphB4-negative arteries were enlarged in *Sox17Δ/Δ* mouse lungs. Insets show higher magnification of veins (A–D, G–H) or arteries (E–F). Scale bars, 100 μm. a, Artery; v, vein.

Conditonal deletion of Sox17 does not influence the expression of key regulators of pulmonary vascular development

To gain insight into the transcriptional changes associated with the pulmonary vascular abnormalities observed in *Sox17Δ/Δ* mice, microarray and qPCR analysis were performed on mRNA isolated from CD146(+) endothelial cells sorted from lungs of E18.5 control and *Sox17Δ/Δ* embryos. mRNAs for *Sox17* and endothelial-specific genes *Mcam/CD146*, *Pecam1*, *Kdr/Vegfr2*, and *Tek/Tie2* were highly enriched in the CD146(+) cell population compared to CD146(-) cells isolated from E18.5 mouse lungs (Supplemental Fig. 4). *Sox17* mRNA was significantly decreased in CD146(+) endothelial cells isolated from *Sox17Δ/Δ* mouse lungs compared to controls, consistent with immunostains showing extensive loss of endothelial Sox17 following *Dermo1-Cre* targeting (Figs. 2 and 5). Expression of *calcium/calmodulin-dependent protein kinase type IV* (*Camk4*), a gene associated with hypertension (Santulli et al., 2012), was significantly decreased in CD146(+) endothelial cells isolated from *Sox17Δ/Δ* mouse lungs (Fig. 5). A modest, but statistically significant increase in *Sox7* mRNA was detected in CD146(+) lung endothelial cells from *Sox17Δ/Δ* embryos, consistent with a potential compensatory increase in the expression other SoxF mRNAs following deletion of *Sox17* (Fig. 5). Aside from these transcriptional changes, microarray and qPCR analysis did not reveal consistent differences in the expression of mRNAs encoding a number of important regulators of blood vessel development or other vascular-related genes in endothelial cells from E18.5 *Sox17Δ/Δ* embryo lungs compared

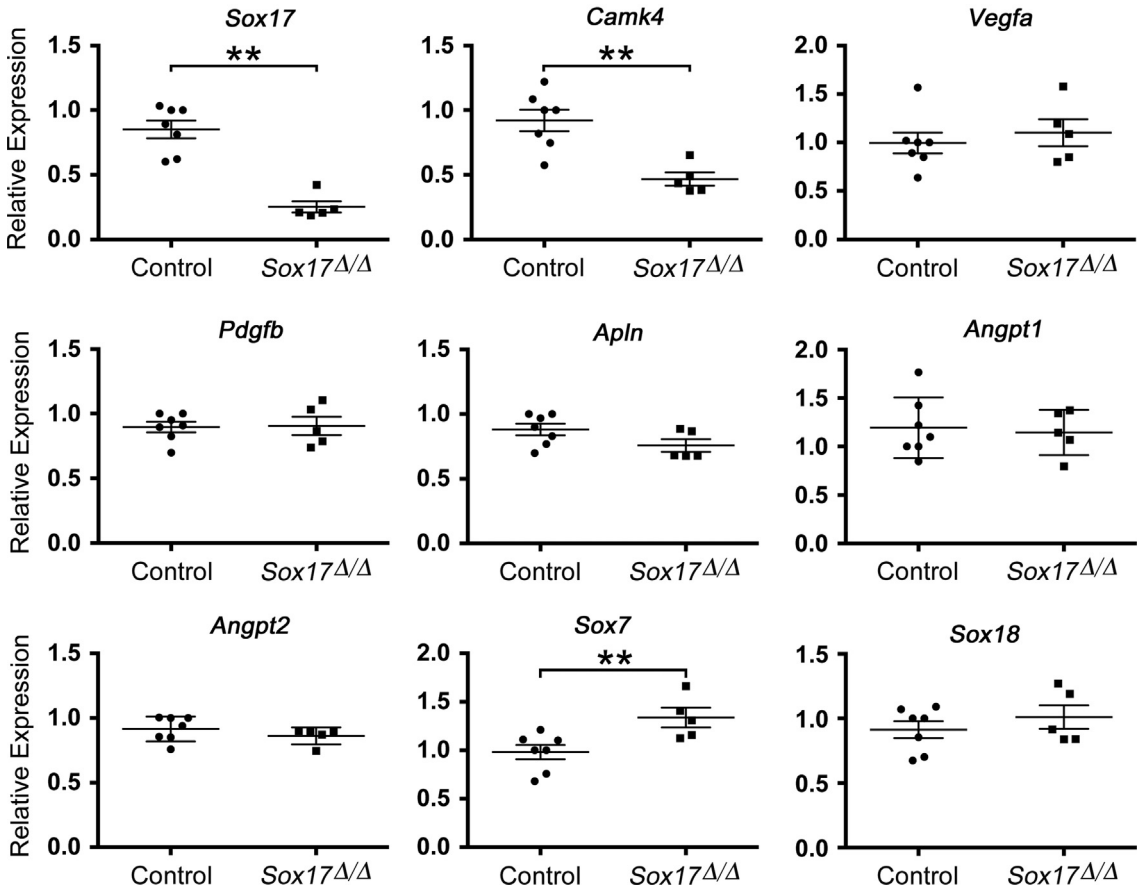

Fig. 5. *Sox17* deletion does not influence the expression of genes known to regulate vascular development. Gene expression was assessed by qPCR using mRNA isolated from CD146(+) endothelial cells harvested from E18.5 control ($n=7$) and *Sox17Δ/Δ* ($n=5$) mouse lungs. *Sox17* and *Camk4* expression was significantly decreased, and *Sox7* mRNA was increased in the CD146(+) endothelial cell population from *Sox17Δ/Δ* lungs compared to controls. Expression of known regulators of vascular morphogenesis and blood vessel size was not affected.

to controls (Fig. 5 and Supplemental data). While endothelial cell heterogeneity and phenotypic variability may have confounded these analyses, these findings suggest that transcriptional changes occurring at earlier developmental time points may underlie the pulmonary vascular abnormalities observed at E18.5 in *Sox17Δ/Δ* mouse lungs.

Pulmonary vascular anomalies and dilated cardiomyopathy are correlated in postnatal Sox17Δ/Δ mice

While pulmonary vascular resistance is high and blood flow is low in the fetal lung, the closure of the fetal cardiovascular circulatory shunts at birth, the rapid growth of alveolar structures, and adjustment to postnatal ventilation are associated with increased cardiopulmonary blood flow and decreased pulmonary vascular resistance. Since the majority of *Sox17Δ/Δ* mice died acutely by 3 weeks of age without antecedent symptoms, cardiovascular abnormalities were assessed in surviving mice at 2 weeks of age. Although body weight of *Sox17Δ/Δ* mice was reduced at E18.5, no differences in the weights of control and *Sox17Δ/Δ* mice were observed at 2 weeks (Supplemental Table 1). Consistent with observations in E18.5 *Sox17Δ/Δ* embryos, dilation of pulmonary arteries and veins was observed in the lungs of *Sox17Δ/Δ* mice at 2 weeks (Fig. 6A and C). Since microCT showed decreased perfusion of the lung microvasculature in E18.5 *Sox17Δ/Δ* embryos, the structure of the pulmonary microvascular network was assessed in 2 week old mice by immunostaining for endomucin and alpha-smooth muscle actin. Endomucin was detected endothelial cells comprising the pulmonary microvasculature and alpha-smooth muscle actin was observed surrounding larger pulmonary blood vessels (Fig. 6D and I). Whole mount staining and confocal microscopy of thick lung sections (150 μm) showed that the endomucin-positive microvasculature was reduced in a subset of surviving *Sox17Δ/Δ* mice at 2 weeks (Fig. 6D and F). Imaging software was used to generate three-dimensional surface representations of the pulmonary microvascular network from the whole mount endomucin staining (Supplemental Fig. 6 and Supplemental movies 3 and 4) and quantitate the area and volume of the lung microvasculature. The pulmonary microvascular area and volume were decreased in *Sox17Δ/Δ* mice at 2 weeks of age (Fig. 2M). Immunofluorescent staining of thin lung sections (10 μm) showed that paucity of the endomucin-positive peripheral microvascular network was associated with alveolar simplification in postnatal *Sox17Δ/Δ* mice (Fig. 6G and I).

While cardiac morphology and size were not affected at E18.5, a subset of *Sox17Δ/Δ* mice had markedly enlarged hearts compared to controls at 2 weeks (Fig. 6J- L and Supplemental Fig. 3). Quantitative analysis of ventricular weights demonstrated that both the right and left ventricles of the heart were significantly enlarged (Fig. 6N). Echocardiographic measurements demonstrated significantly increased systolic/diastolic LV internal dimensions and echocardiographically-derived LV mass in *Sox17Δ/Δ* mice (Table 2). Shortening fraction was not altered, demonstrating that there was no difference in systolic function, and tissue Doppler of the MV annulus revealed no compromise of diastolic function. Notably, *Sox17Δ/Δ* mice had a higher incidence of

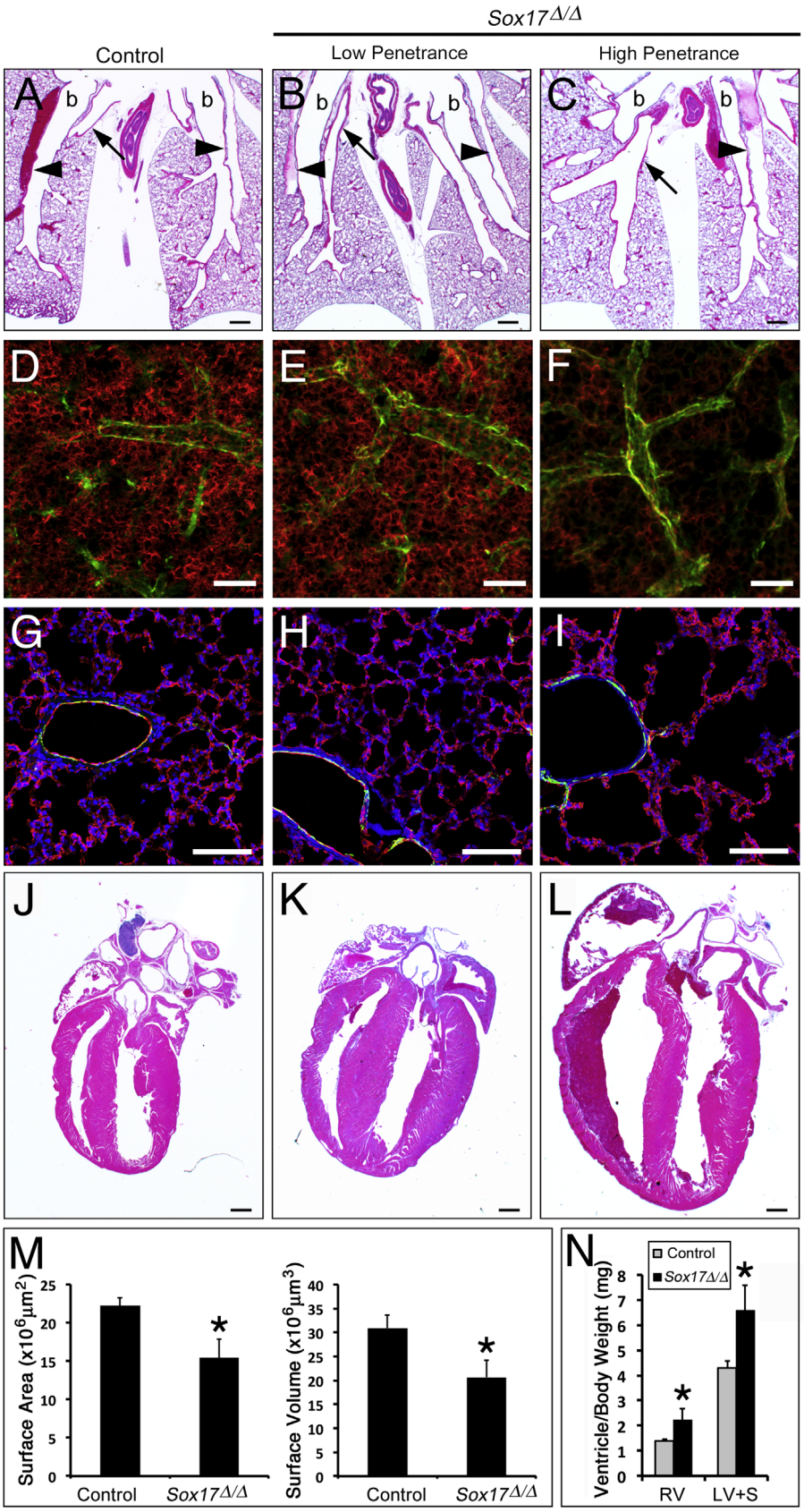

Fig. 6. Postnatal *Sox17Δ/Δ* mice with pulmonary vascular abnormalites develop enlarged hearts. (A–C) Histological analysis of lungs from 2 week old control (A) and *Sox17Δ/Δ* (B–C) mice shows variable enlargement of pulmonary blood vessels. arrowheads, arteries; arrows, veins; b, bronchus. (D–I) Immunofluorescence staining for endomucin (red) and alpha-smooth muscle actin (green) was performed on lung sections from 2 week old control (D and G) and *Sox17Δ/Δ* (E and F, H and I) mice. (D-F) Whole mount staining of thick sections (150 μm) showed that the endomucin-positive microvascular network was variably reduced in the lungs of *Sox17Δ/Δ* mice. (G-I) Immunofluorescence staining of thin lung sections (10 μm) showed that paucity of the microvasculature was associated with alveolar simplification in severely affected *Sox17Δ/Δ* mice. (M) The area and volume of the pulmonary vascular network determined from endomucin staining were decreased in *Sox17Δ/Δ* mice. (J–L) Histological analysis of hearts from 2 week old control (J) and *Sox17Δ/Δ* (K and L) mice shows variable cardiac enlargement. (N) Ventricle weights were significantly increased in 2 week old *Sox17Δ/Δ* mice compared to controls. RV, right ventricle; LV+S, left ventricle and septum. The severity of pulmonary vascular abnormalities and heart enlargement in *Sox17Δ/Δ* mice were well correlated. Scale bars 500 μm (A–C and J–L); 100 μm (D–I). Asterisks indicated statistical significance as determined by Student's *t*-test ($p \leq .05$).

Table 2
Echocardiography data.

	Control ($n=7$)	*Sox17* Δ/Δ ($n=10$)
IVSd (mm)	.56 ± .10	.63 ± .09
LVPWd (mm)	.52 ± .06	.59 ± .09
LA (mm)	1.97 ± .29	2.45 ± .78
LVIDd (mm)	3.39 ± .26	4.05 ± .59
LVIDs (mm)	2.29 ± .39	2.74 ± .40**
SF (%)	33 ± 7	32 ± 5
LVM (mg)	42 ± 6	71 ± 27**
Heart rate (bpm)	366 ± 79	336 ± 48

IVSd, interventricular septum thickness in diastole; LA, left atrial dimension; LVPWd, left ventricular posterior wall in diastole; LVIDd, left ventricular internal dimension in diastole; LVIDs, left ventricular internal dimension in systole; SF, shortening fraction; LVM, left ventricular mass.

** $p < .05$; Student's *t*-test.

atrioventricular valve regurgitation. While regurgitation of the mitral and tricuspid valves was not observed in control mice (0/7), 40% of *Sox17* deficient mice (4/10) had detectable regurgitation of both atrioventricular valves (Supplemental Fig. 5 and Supplemental Table 2). Despite the presence of valve regurgitation, there were no differences in antegrade flow velocities between control and Sox17 deficient mice. The severity of pulmonary vascular and cardiac abnormalities observed at 2 weeks were correlated, wherein *Sox17Δ/Δ* mice with more severely dilated pulmonary veins/arteries and reduced microvascular networks also had larger hearts and valve regurgitation (Fig. 6 and Supplemental Table 2).

Dermo1-Cre directs recombination in the developing heart, including the epicardium, perivascular cells, and interstitial cells of the valve leaflets (Supplemental Fig. 1) (Lavine et al., 2008). In the embryonic and postnatal heart, Sox17 staining was detected in coronary vascular and intramyocardial endothelial cells, and in rare endocardial cells lining the valve leaflets, which did not overlap with *Dermo1-Cre* lineage-labeled cells (Supplemental Fig. 3). Sox17 mRNA and immunostaining were not significantly altered in the hearts of E18.5 or postnatal *Sox17Δ/Δ* mice (Supplemental Fig. 3). These observations indicate that cardiac cells derived from the *Dermo1-Cre* lineage and Sox17-expressing endothelial cells in the heart are predominantly separate cell populations. However, we cannot exclude the possibility that a rare subset of Sox17-positive endothelial cells in the heart may be targeted by *Dermo1-Cre*. While these data indicate that the cardiac defects observed in postnatal *Sox17Δ/Δ* mice were not associated with substantial loss of Sox17 in heart tissue, cardiac dysfunction and failure are likely the cause of death in *Sox17Δ/Δ* mice.

Discussion

Conditional deletion of *Sox17* from endothelial cells within the embryonic lung mesenchyme caused abnormal morphogenesis of the pulmonary vasculature, including the formation of pulmonary vein varices, enlarged arteries, and a variably reduced microvasculature. The severity of the pulmonary vascular abnormalities in *Sox17Δ/Δ* mice was correlated with the postnatal development of dilated cardiomyopathy, causing death at 3–4 weeks of age. These data demonstrate that Sox17 is required in endothelial cells of the developing lung for normal pulmonary vascular morphogenesis and postnatal cardiopulmonary circulatory function.

Following conditional inactivation of *Sox17* with *Dermo1Cre*, the majority of *Sox17Δ/Δ* mice died acutely during the postnatal period between birth and 3 weeks. Pulmonary vein varix, the most consistent vascular anomaly observed in *Sox17Δ/Δ* mice, is typically an asymptomatic condition in humans and is an unlikely cause of lethality in the *Sox17Δ/Δ* mice (Ben-menachem et al., 1975). Further, neither hemorrhage nor pulmonary vascular congestion was observed in the lungs of embryonic or postnatal *Sox17Δ/Δ* mice despite the abnormal dilation of pulmonary blood vessels and microvascular defects, indicating that pulmonary vascular integrity is maintained. While vascular networks are established during embryogenesis, the blood flow and hemodynamics in the fetal and postnatal circulatory systems are distinct, and dramatic changes in the cardiopulmonary circulation occur at birth. In the fetal circulation, blood flow through the lung is low and pulmonary vascular resistance is high. At birth, the closure of fetal circulatory shunts and the transition to air breathing is associated with a rapid decrease in pulmonary vascular resistance and a marked increase in pulmonary blood flow. Abnormal formation and circulatory function of the pulmonary vasculature, in clinical conditions such as bronchopulmonary dysplasia and pulmonary hypertension, contribute to cardiac dysfunction and failure. Conditional deletion of Sox17 from endothelial cells in the developing lung caused pulmonary vascular abnormalities, including enlarged macrovascular blood vessels and a diminished microvascular network. While endothelial cell differentiation in the lungs of *Sox17Δ/Δ* mice was unaffected at E18.5, hypoperfusion of the peripheral microvasculature observed by microCT suggests decreased blood flow through the pulmonary vasculature. Since hemodynamic forces influence endothelial cell survival and homeostasis (Chiu and Chien, 2011), reduced pulmonary vascular blood flow in *Sox17Δ/Δ* mice may contribute to the paucity of the microvascular network detected 2 weeks. While vascular abnormalities were only histologically apparent in the lungs and not other organs of fetal *Sox17Δ/Δ* mice, these mice developed biventricular hypertrophy and atrioventricular valve regurgitation at 2 weeks of age. Sox17 was extensively deleted from vascular endothelial cells in the lung, whereas changes in the expression of Sox17 were not detectable in cardiac tissues, including the valves and coronary vessels of fetal or postnatal *Sox17Δ/Δ* mice. While Sox17 expression and *Dermo1-Cre* mediated recombination were observed in cardiac tissue, they did not overlap at the cellular level. Although primary cardiac dysfunction cannot be excluded, the finding that Sox17 expression was maintained in the heart indicates that the cardiac phenotype in *Sox17Δ/Δ* mice is likely secondary to impairment of the cardiopulmonary circulation. The paucity of the lung microvasculature observed in postnatal *Sox17Δ/Δ* mice is likely to cause pulmonary hypertension and, in turn, cardiac hypertrophy and failure. While pulmonary hypertension primarily affects the right heart, both right and left ventricular hypertrophy was observed in *Sox17Δ/Δ* mice. Sustained increases in pressure and volume on the right ventricle in chronic pulmonary hypertension can lead to biventricular remodeling and dysfunction (Voelkel et al., 2006). While systemic hypertension is a potential alternative cause of the biventricular cardiac hypertrophy, vascular abnormalities in organs other than the lung were not observed following conditional deletion of *Sox17*. Although systemic hypertension cannot be excluded, our data support the concept that abnormal prenatal and postnatal morphogenesis of the pulmonary vascular network in *Sox17Δ/Δ* mice results in a paucity of microvascular cells that impairs the pulmonary circulation, leading to dilated cardiomyopathy and death in postnatal *Sox17Δ/Δ* mice.

The present study shows that Sox17 is restricted to endothelial cells of the pulmonary arteries, veins, and microvasculature in the embryonic and postnatal lung. These observations are consistent with the endothelial-specific expression of a Sox17-mCherry fusion protein in the embryonic lung of a knock-in reporter mouse model and lineage labeling of the vascular endothelium by *Sox17-Cre*

knock-in mice (Burtscher et al., 2012; Choi et al., 2012; Engert et al., 2013; Engert et al., 2009; Liao et al., 2009). Staining for Sox17 in the pulmonary vasculature was stronger in artery and microvascular endothelial cells compared to veins, consistent with Sox17 expression in other vascular systems (Corada et al., 2013; Liao et al., 2009). While Sox17 is transiently expressed in endodermal progenitor cells prior to the emergence of the lung primordium, it is not detected in the endoderm-derived respiratory epithelium thereafter (Engert et al., 2013; Lange et al., 2009). Although Sox17 immunostaining was previously observed in respiratory epithelial cells of the embryonic and postnatal lung, *Sox17* mRNA was not detected in pulmonary epithelial cells (Park et al., 2006). Thus, it is likely that the previous Sox17 staining in the respiratory epithelium was related to antisera cross-reactivity, potentially to other Sox family members.

Dermo1-Cre is active in foregut mesenchyme at E9.5 and directs recombination in the mesenchyme and mesothelium of the embryonic lung (Cornett et al., 2013; Yin et al., 2008). Multiple cell types are derived from the embryonic lung mesenchyme, including fibroblasts, pericytes, smooth muscle, and pulmonary vascular endothelial cells. While the extent of *Dermo1-Cre* mediated recombination in endothelial cells of the developing lung from published studies is unclear (De Langhe et al., 2008; Morimoto et al., 2010; Tiozzo et al., 2012; White et al., 2007; Yin et al., 2008), we show that conditional deletion of *Sox17* using *Dermo1-Cre* resulted in extensive loss of Sox17 expression in endothelial cells of the developing lung, causing abnormalities of the pulmonary vasculature. In *Sox17Δ/Δ* embryos, *Sox17* mRNA expression in lung endothelial cells was reduced to approximately 30% of controls. These data demonstrate that *Dermo1-Cre* directs substantial, but incomplete recombination in endothelial cells derived from the developing lung mesenchyme. Whether the subset of lung endothelial cells that were not targeted by *Dermo1-Cre* are derived from cells of distinct embryonic origins or are specified from progenitors prior to the onset of Cre activity is unclear. Conditional deletion of *Pten* or β-*catenin* using *Dermo1-Cre* caused defects in angioblast differentiation into endothelial cells, supporting the concept that *Dermo1-Cre* likely targets the endothelial lineage at the angioblast progenitor stage (De Langhe et al., 2008; Tiozzo et al., 2012). *Dermo1-Cre* mediated recombination of endothelial cells of the developing lung will be a useful tool to gain insights into the molecular mechanisms that govern pulmonary vascular morphogenesis.

While pulmonary vascular abnormalities were histologically apparent in *Sox17Δ/Δ* mice, endothelial cell differentiation was relatively unaltered and substantial transcriptional changes in gene expression profiles were not detected in pulmonary endothelial cells isolated from *Sox17Δ/Δ* embryos at E18.5. The lack of differences in mRNA expression following conditional deletion of Sox17 suggests that transcriptional changes that contributed to the abnormal vascular morphogenesis in the lungs of *Sox17Δ/Δ* embryos likely occurred at earlier developmental stages. Alternatively, mosaic deletion of Sox17 and phenotypic variability among *Sox17Δ/Δ* mice may have confounded the analyses. Yang et. al. also reported relatively few changes in mRNA microarray expression profiles following siRNA-mediated knockdown of Sox17 in primary endothelial cells in culture (Yang et al., 2013). Recent studies support a role for Sox17 upstream of the Notch pathway in regulating arterial endothelial cell differentiation and vascular remodeling (Corada et al., 2013). Thus, while Sox17 is required for normal development of the pulmonary vasculature, the transcriptional targets of Sox17 in lung endothelial cells remain to be determined. In adult mice, Sox17 is widely expressed in pulmonary vascular endothelial cells. However, its potential role in regulating pulmonary vascular homeostasis and remodeling in the mature lung is not known.

Funding sources

The present work was supported by Grants NIH HL090156 and HL110964 Lung Regeneration and Repair Consortium (LRRC) (J.A.W.), the Medical Research Council Clinician Scientist Fellowship G0802804, (H.M.H.; London, UK) and a Postgraduate Research Student Scholarship (N.U.; University of Southampton).

Acknowledgments

The authors would like to thank Marc Lubitz, Gail Macke and Paula Blair for their assistance with histology and imaging, the CICRL/mouse echocardiography core, and Dr. Ron Pratt from the CCHMC Imaging Research Center for obtaining and reconstructing the microCT images.

Appendix A. Supporting information

Supplementary data associated with this article can be found in the online version at http://dx.doi.org/10.1016/j.ydbio.2013.11.018.

References

Acehan, D., Vaz, F., Houtkooper, R.H., James, J., Moore, V., Tokunaga, C., Kulik, W., Wansapura, J., Toth, M.J., Strauss, A., Khuchua, Z., 2011. Cardiac and skeletal muscle defects in a mouse model of human barth syndrome. J. Biol. Chem. 286, 899–908.

Ahnfelt-Ronne, J., Jorgensen, M.C., Hald, J., Madsen, O.D., Serup, P., Hecksher-Sorensen, J., 2007. An improved method for three-dimensional reconstruction of protein expression patterns in intact mouse and chicken embryos and organs. J. Histochem. Cytochem. 55, 925–930.

Ben-menachem, Y., Kuroda, K., Kyger , E.R., Brest, A.N., Copeland, O.P., Coan, J.D., 1975. The various forms of pulmonary varices. report of three cases and review of the literature. Am. J. Roentgenol. Radium Ther. Nucl. Med. 125, 881–889.

Brachtendorf, G., Kuhn, A., Samulowitz, U., Knorr, R., Gustafsson, E., Potocnik, A.J., Fassler, R., Vestweber, D., 2001. Early expression of endomucin on endothelium of the mouse embryo and on putative hematopoietic clusters in the dorsal aorta. Dev. Dyn. 222, 410–419.

Burtscher, I., Barkey, W., Schwarzfischer, M., Theis, F.J., Lickert, H., 2012. The Sox17-mCherry fusion mouse line allows visualization of endoderm and vascular endothelial development. Genesis 50, 496–505.

Cermenati, S., Moleri, S., Cimbro, S., Corti, P., Del Giacco, L., Amodeo, R., Dejana, E., Koopman, P., Cotelli, F., Beltrame, M., 2008. Sox18 and Sox7 play redundant roles in vascular development. Blood 111, 2657–2666.

Chiu, J.J., Chien, S., 2011. Effects of disturbed flow on vascular endothelium: pathophysiological basis and clinical perspectives. Physiol. Rev. 91, 327–387.

Choi, E., Kraus, M.R., Lemaire, L.A., Yoshimoto, M., Vemula, S., Potter, L.A., Manduchi, E., Stoeckert , C.J., Grapin-Botton, A., Magnuson, M.A., 2012. Dual lineage-specific expression of Sox17 during mouse embryogenesis. Stem Cells 30, 2297–2308.

Clarke, R.L., Yzaguirre, A.D., Yashiro-Ohtani, Y., Bondue, A., Blanpain, C., Pear, W.S., Speck, N.A., Keller, G., 2013. The expression of Sox17 identifies and regulates haemogenic endothelium. Nat. Cell Biol. 15, 502–510.

Corada, M., Orsenigo, F., Morini, M.F., Pitulescu, M.E., Bhat, G., Nyqvist, D., Breviario, F., Conti, V., Briot, A., Iruela-Arispe, M.L., Adams, R.H., Dejana, E., 2013. Sox17 is indispensable for acquisition and maintenance of arterial identity. Nat. Commun. 4, 2609.

Cornett, B., Snowball, J., Varisco, B.M., Lang, R., Whitsett, J., Sinner, D., 2013. Wntless is required for peripheral lung differentiation and pulmonary vascular development. Dev. Biol. 1, 38–52.

De Langhe, S.P., Carraro, G., Tefft, D., Li, C., Xu, X., Chai, Y., Minoo, P., Hajihosseini, M. K., Drouin, J., Kaartinen, V., Bellusci, S., 2008. Formation and differentiation of multiple mesenchymal lineages during lung development is regulated by beta-catenin signaling. PLoS One 3, e1516.

Degenhardt, K., Wright, A.C., Horng, D., Padmanabhan, A., Epstein, J.A., 2010. Rapid 3d phenotyping of cardiovascular development in mouse embryos by micro-ct with iodine staining. Circ. Cardiovasc. Imaging 3, 314–322.

Engert, S., Burtscher, I., Kalali, B., Gerhard, M., Lickert, H., 2013. The Sox17 CreERT2 knock-in mouse line displays spatiotemporal activation of Cre recombinase in distinct Sox17 lineage progenitors. Genesis 51, 793–802.

Engert, S., Liao, W.P., Burtscher, I., Lickert, H., 2009. Sox17-2a-Icre: a knock-in mouse line expressing cre recombinase in endoderm and vascular endothelial cells. Genesis 47, 603–610.

Francois, M., Caprini, A., Hosking, B., Orsenigo, F., Wilhelm, D., Browne, C., Paavonen, K., Karnezis, T., Shayan, R., Downes, M., Davidson, T., Tutt, D., Cheah, K.S., Stacker, S.A., Muscat, G.E., Achen, M.G., Dejana, E., Koopman, P., 2008.

Sox18 induces development of the lymphatic vasculature in mice. Nature 456, 643–647.
Galambos, C., deMello, D.E., 2007. Molecular mechanisms of pulmonary vascular development. Pediatr. Dev. Pathol. 10, 1–17.
Herpers, R., van de Kamp, E., Duckers, H.J., Schulte-Merker, S., 2008. Redundant roles for Sox7 and Sox18 in arteriovenous specification in zebrafish. Circ. Res. 102, 12–15.
Irrthum, A., Devriendt, K., Chitayat, D., Matthijs, G., Glade, C., Steijlen, P.M., Fryns, J.P., Van Steensel, M.A., Vikkula, M., 2003. Mutations in the transcription factor gene Sox18 underlie recessive and dominant forms of hypotrichosis–lymphedema–telangiectasia. Am. J. Hum. Genet. 72, 1470–1478.
Kanai-Azuma, M., Kanai, Y., Gad, J.M., Tajima, Y., Taya, C., Kurohmaru, M., Sanai, Y., Yonekawa, H., Yazaki, K., Tam, P.P., Hayashi, Y., 2002. Depletion of definitive gut endoderm in Sox17-Null mutant mice. Development 129, 2367–2379.
Kim, I., Saunders, T.L., Morrison, S.J., 2007. Sox17 dependence distinguishes the transcriptional regulation of fetal from adult hematopoietic stem cells. Cell 130, 470–483.
Lange, A.W., Keiser, A.R., Wells, J.M., Zorn, A.M., Whitsett, J.A., 2009. Sox17 promotes cell cycle progression and inhibits Tgf-Beta/Smad3 signaling to initiate progenitor cell behavior in the respiratory epithelium. PLoS One 4, e5711.
Lavine, K.J., Long, F., Choi, K., Smith, C., Ornitz, D.M., 2008. Hedgehog signaling to distinct cell types differentially regulates coronary artery and vein development. Development 135, 3161–3171.
Liao, W.P., Uetzmann, L., Burtscher, I., Lickert, H., 2009. Generation of a mouse line expressing Sox17-driven cre recombinase with specific activity in arteries. Genesis 47, 476–483.
Matsui, T., Kanai-Azuma, M., Hara, K., Matoba, S., Hiramatsu, R., Kawakami, H., Kurohmaru, M., Koopman, P., Kanai, Y., 2006. Redundant roles of Sox17 and Sox18 in postnatal angiogenesis in mice. J. Cell Sci. 119, 3513–3526.
Morimoto, M., Liu, Z., Cheng, H.T., Winters, N., Bader, D., Kopan, R., 2010. Canonical notch signaling in the developing lung is required for determination of arterial smooth muscle cells and selection of clara versus ciliated cell fate. J. Cell Sci. 123, 213–224.
Park, K.S., Wells, J.M., Zorn, A.M., Wert, S.E., Whitsett, J.A., 2006. Sox17 influences the differentiation of respiratory epithelial cells. Dev. Biol. 294, 192–202.
Pendeville, H., Winandy, M., Manfroid, I., Nivelles, O., Motte, P., Pasque, V., Peers, B., Struman, I., Martial, J.A., Voz, M.L., 2008. Zebrafish Sox7 and Sox18 function together to control arterial–venous identity. Dev. Biol. 317, 405–416.
Sakamoto, Y., Hara, K., Kanai-Azuma, M., Matsui, T., Miura, Y., Tsunekawa, N., Kurohmaru, M., Saijoh, Y., Koopman, P., Kanai, Y., 2007. Redundant roles of Sox17 and Sox18 in early cardiovascular development of mouse embryos. Biochem. Biophys. Res. Commun. 360, 539–544.
Santulli, G., Cipolletta, E., Sorriento, D., Del Giudice, C., Anastasio, A., Monaco, S., Maione, A.S., Condorelli, G., Puca, A., Trimarco, B., Illario, M., Iaccarino, G., 2012. Camk4 gene deletion induces hypertension. J. Am. Heart Assoc. 1, e001081.
Spence, J.R., Lange, A.W., Lin, S.C., Kaestner, K.H., Lowy, A.M., Kim, I., Whitsett, J.A., Wells, J.M., 2009. Sox17 regulates organ lineage segregation of ventral foregut progenitor cells. Dev. Cell 17, 62–74.
Tiozzo, C., Carraro, G., Al Alam, D., Baptista, S., Danopoulos, S., Li, A., Lavarreda-Pearce, M., Li, C., De Langhe, S., Chan, B., Borok, Z., Bellusci, S., Minoo, P., 2012. Mesodermal pten inactivation leads to alveolar capillary dysplasia-like phenotype. J. Clin. Invest. 122, 3862–3872.
Voelkel, N.F., Quaife, R.A., Leinwand, L.A., Barst, R.J., McGoon, M.D., Meldrum, D.R., Dupuis, J., Long, C.S., Rubin, L.J., Smart, F.W., Suzuki, Y.J., Gladwin, M., Denholm, E.M., Gail, D.B., 2006. Right ventricular function and failure: report of a national heart, lung, and blood institute working group on cellular and molecular mechanisms of right heart failure. Circulation 114, 1883–1891.
White, A.C., Lavine, K.J., Ornitz, D.M., 2007. Fgf9 and Shh regulate mesenchymal vegfa expression and development of the pulmonary capillary network. Development 134, 3743–3752.
White, A.C., Xu, J., Yin, Y., Smith, C., Schmid, G., Ornitz, D.M., 2006. Fgf9 and Shh signaling coordinate lung growth and development through regulation of distinct mesenchymal domains. Development 133, 1507–1517.
Yang, H., Lee, S., Lee, S., Kim, K., Yang, Y., Kim, J.H., Adams, R.H., Wells, J.M., Morrison, S.J., Koh, G.Y., Kim, I., 2013. Sox17 promotes tumor angiogenesis and destabilizes tumor vessels in mice. J. Clin. Invest. 123, 418–431.
Yin, Y., White, A.C., Huh, S.H., Hilton, M.J., Kanazawa, H., Long, F., Ornitz, D.M., 2008. An Fgf-Wnt gene regulatory network controls lung mesenchyme development. Dev. Biol. 319, 426–436.
Yu, K., Xu, J., Liu, Z., Sosic, D., Shao, J., Olson, E.N., Towler, D.A., Ornitz, D.M., 2003. Conditional inactivation of fgf receptor 2 reveals an essential role for Fgf Signaling in the regulation of osteoblast function and bone growth. Development 130, 3063–3074.